JOURNAL OF CATALYSIS 149, 247–253 (1994)

Decarbonylation and CO Adsorption on Cluster-Derived Iron Catalyst: Surface Formation and Coordinate Geometry of $Fe_3(CO)_6(\mu_3\text{-}CO)/Al_2O_3$

Yuan Kou,[1] Zhang-Huai Suo, and Hong-Li Wang

State Key Laboratory for Oxo Synthesis and Selective Oxidation, Lanzhou Institute of Chemical Physics, Chinese Academy of Sciences, Lanzhou 730000, China

Received February 22, 1993; revised April 15, 1994

A surface species has been formed on the cluster-derived catalyst Fe/Al_2O_3 by saturation with CO. Fe *K*-edge extended X-ray absorption fine structure (EXAFS) analysis reveals a contribution from the colinear Fe–C–O array as well as a formula of $Fe_3(CO)_6(\mu_3\text{-}CO)/Al_2O_3$ with C_{3v} symmetry for the species. The bond lengths of Fe–C_t (C_t = terminal carbon), Fe–μ_3-C, Fe–O, and Fe–Fe are 1.84(3), 1.96(1), 1.96(1), and 2.48(6) Å, respectively. The angle Fe–μ_3-C–Fe is about 80° and that between the Fe–μ_3-C bond and the Fe_3 plane is about 42°. The geometric consideration reveals that the species is inlaid into the surface and stabilized by the Fe(μ_3-C) (μ_3-O) core. Introducing the basic concept of coordination chemistry to the surface approach, the species can be described as $[Fe_3(CO)_6(\mu_3\text{-}CO)(O)_6(\mu_3\text{-}O)]^{3-}$, a molecular anion with C_{3v} symmetry ionically bound to the Al^+ cationic site. The results suggest that formation of an active intermediate with a μ_3 carbide ligand from the μ_3-CO is geometrically allowed, but it is unlikely that it can give high activity in CO hydrogenation because of the stability of the Fe(μ_3-C)(μ_3-O) core. © 1994 Academic Press, Inc.

I. INTRODUCTION

Studies of ensembles of several metal atoms on a surface (1, 2) are, in principle, based on the hypothesis that a catalytic cycle cannot occur at a single surface metal atom (3) and, in practice, are stimulated by the fact that CO activation is well understood in carbonyl chemistry (4). The preparation and characterization of highly dispersed Fe/Al_2O_3 catalyst derived from precipitated $Fe_3(CO)_{12}$ provide an opportunity to produce tri-iron carbonyl species on the surface. The Fe/Al_2O_3 exhibits good selectivity for lower olefins in the hydrogenation of CO. Characterization of Fe/Al_2O_3 by *K*-edge X-ray absorption spectroscopy (XAS) has demonstrated that the active site on the surface is an ensemble of three iron atoms (5). Although the aggregation of these Fe_3 ensembles to groups larger than 10 Å brings about poor selectivity for the catalyst after use, the ensemble of three irons is still retained. The aggregating process favored by the surface of Al_2O_3, in fact, is the aggregation of several iron ensembles.

Maintaining the white sample Fe/Al_2O_3(K7) in a CO atmosphere gave a yellow product (K7CO) and caused the reappearance of three weak infrared absorptions at 2047, 2014, and 1549 cm^{-1} (5). One of the problems is whether the coordinate geometry and structure of the surface species differ from those of any known product obtained by a synthetic route. Generally, one can easily estimate that any surface molecule-like species cannot be simply obtained by removing the CO ligands from the bottom of the tri-iron plane occupied by surface oxygens. This paper reports the results of an Fe *K*-edge XAS study of K7CO, with emphasis on the surface geometry of the species.

II. EXPERIMENTAL

All operations and characterizations were performed strictly without exposure to oxygen or moisture.

Preparation of $Fe_3(CO)_{12}/Al_2O_3$. $Fe_3(CO)_{12}/Al_2O_3$ was prepared by a novel method, precipitating the cluster on γ-Al_2O_3:

$$3HFe(CO)_4^- + 3MnO_2 + 3H_2O \longrightarrow \text{rosy solution} \xrightarrow{Al_2O_3} \text{impregnated } Al_2O_3 \xrightarrow{H^+} Fe_3(CO)_{12}/Al_2O_3$$

The details are available in Ref. (5).

Decarbonylation and adsorption of CO. The freshly prepared $Fe_3(CO)_{12}/Al_2O_3$ (0.9 wt% Fe) was treated *in vacuo* at 310 K overnight and then up to 420 K for 4 h. The resulting white sample Fe/Al_2O_3, which had no infrared absorption band due to a carbonyl group in the range 2200 to 1400 cm^{-1}, was then maintained in a CO

[1] To whom correspondence should be addressed.

0021-9517/94 $6.00

atmosphere for a few days to give the yellow product K7CO which showed several weak infrared absorption bands at 2047, 2014 and 1556, 1542, 1520 cm^{-1} (previously observed values were 2047, 2014, and 1549 cm^{-1}).

Hydrogenation of CO was carried out in a fixed-bed reactor with an *in situ* GC analyzer under the following conditions: 2.0 MPa syngas ($CO : H_2 = 1 : 2$), 473 K, and GHSV = 600–1000 h^{-1}.

Spectral measurement. Infrared measurement was recorded on a Fourier transform Nicolet 10DX spectrometer using a Nujol mull for pure $Fe_3(CO)_{12}$ and pressed disk for $Fe_3(CO)_{12}/Al_2O_3$. *In situ* infrared spectra were checked by subtraction of the background of Al_2O_3 but are presented without it to remove any doubt concerning the validity of the spectral assignment.

X-ray absorption spectra were obtained in fluorescence mode using the BL-7C facility at the Photon Factory (Tsukuba, Japan). A Si(111) double-crystal (sagittal focusing) monochromator with a position beam energy of 2.5 GeV and an average stored current of 250 mA was employed. Spectra were recorded in four energy regions about the Fe *K*-edge, −100 to −30 eV in 15-eV steps, −30 to 70 eV in 0.5-eV steps, 70 to 700 eV in 4-eV steps, and above 700 eV in 8-eV steps. The signal was integrated for 4 s at each point. The sample of K7 maintained under N_2 and that of K7CO maintained under CO were sealed in flasks for performing the XAS measurement. Specimens were made by directly applying the fine powders to Scotch tape inside a glove box kept under an atmosphere of N_2, sealed by the tape, and then measured immediately.

Data analysis. The data were processed on a 386 microcomputer with the Program Library for EXAFS Data Analysis written by the Institute of Physics, Chinese Academy of Sciences (5). X-ray absorption near edge structure (XANES) data were normalized within 70 eV (−20 to 50 eV) about the edge (6, 7). The absorption threshold E_T used as the zero of energy was taken with respect to the first inflection point, while E_0 was taken at the maximum in the derivative spectrum. Extended X-ray absorption fine structure (EXAFS) data were normalized by a smooth spline μ_0, determined by a cubic spline fit of the continuum above the edge to about 900 eV. The raw data and the resulting spline of K7CO are shown in Fig. 1. The EXAFS oscillation was determined by $\chi(k) = (\mu - \mu_0)/\mu_0$. The $k^3\chi(k)$ was Fourier transformed into *r*-space by a Hanning window function. The procedures were checked several times with different spline parameters and within different *k*-spaces, generally reproduced in the range $k = 3.5$ to 12.0 to make sure that the Fourier transforms obtained for each sample had uniform spectral features.

The Fourier transform containing the peaks of interest was filtered into *k*-space by a Hanning window function.

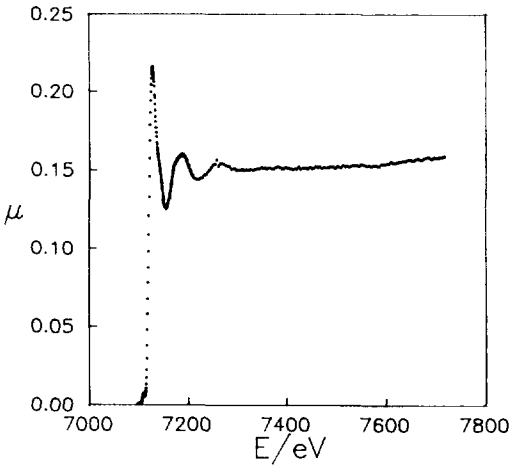

FIG. 1. Raw XAFS data for K7CO.

A least-squares curve-fitting procedure was then performed to calculate the structural parameters for each shell using theoretically calculated components determined by Program FEFF3.25 developed by Rehr and his colleagues (8, 9). The structural parameters [coordination number, (CN), shell radius *R* in Ångstrom units; Debye–Waller factor (DW) in Ångstrom units squared] with which the FEFF was started were corrected repeatedly until they were identical to the fitting parameters. The reduction factor used, S_0^2, was 1.1. The best fit of fitting curves was first chosen by an *R* factor, then was transformed into *r*-space weighted by k^0 with the same range to give a fit of the Fourier transform. The parameter error estimates were calculated by the recommended method (10). The correlations between the variables were estimated by the standard method (11).

III. RESULTS AND DISCUSSION

1. Decarbonylation of $Fe_3(CO)_{12}/Al_2O_3$

The green particles of $Fe_3(CO)_{12}/Al_2O_3$ washed by 0.3 *M* K_2CO_3 solution were dried overnight *in vacuo* at 300 K and then maintained under a nitrogen atmosphere. The decarbonylation thus occurred spontaneously. The lower the metal loading, the more significant the decoloring process observed. After 2 weeks, the green particles with the highest loading (1.1 wt% Fe) changed slightly to pale green, but a portion of the particles with the lowest loading (0.6 wt% Fe) changed to bright yellow. An infrared spectrum of the yellow particles showed only two very broad bands centered at 2086 and 1549 cm^{-1}. The infrared bands centered at 1549 cm^{-1} suggest the presence of ensembles of several iron atoms. It is unlikely that an ensemble is connected to a surface Lewis acidic center by a μ_2-CO ligand (1548 cm^{-1}) because the acidity of γ-Al_2O_3 is not

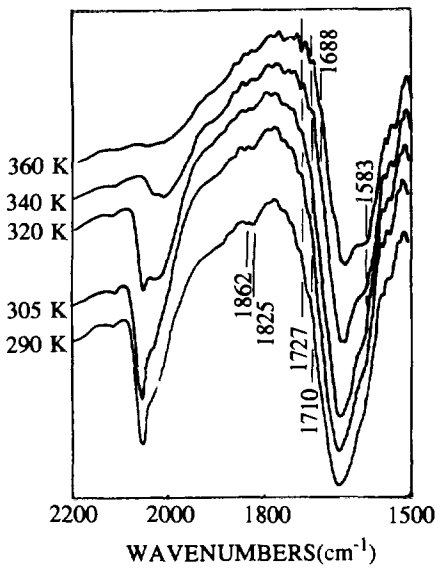

FIG. 2. *In situ* infrared spectra of $Fe_3(CO)_{12}/Al_2O_3$ under decarbonylation conditions (*in vacuo*).

as strong as that of $AlBr_3$ (12). It is quite likely that these low CO stretching frequencies indicate a μ_3-CO ligand connected with an Fe_3 ensemble.

In situ infrared analysis under the decarbonylation conditions (300 to 450 K *in vacuo*) shows that the decarbonylation of terminal groups starts at 320 K and ends at 360 K. However, the disappearance of bridging carbonyls is relatively slow, beginning at 300 K but not ending even up to 400 K (see Fig. 2). During decarbonylation, several new infrared bands at 1727, 1710, 1688, and 1583 cm^{-1} are observed. These bands are tentatively assigned to a face-bridging CO such as 1670 cm^{-1} in $[PPN]_2Fe_3(CO)_{11}$ and 1680 cm^{-1} in $[PPN]_2$ $Fe_4(CO)_{13}$ (13), and/or a bridging CO such as 1639 to 1742 cm^{-1} in $HFe_3(CO)_{11}$ ion (14, 15). *In situ* infrared results reveal that complete disappearance of the bridging bands which range from 1800 to 1500 cm^{-1} requires more severe conditions (30–60 min *in vacuo* at 420 K). It is likely that a remaining μ_3-CO ligand is of particular importance in the stabilization of the Fe_3 core.

2. *CO Adsorption on* Fe/Al_2O_3

The Fourier transform of the *K*-edge EXAFS of Fe/Al_2O_3 saturated with CO (K7CO), compared with that of Fe/Al_2O_3 (K7), is shown in Fig. 3. Several significant changes are found in the spectra, as follows. (i) The intensity of the most intense peak, which was assigned to the O-scatterers in K7, is significantly enhanced due to the addition of C-scatterers in the first coordination sphere. (ii) The third peak has disappeared. This peak and the second peak of the K7 spectrum were assigned to the second and the first Fe neighbors. The intensity of the second peak of the K7CO spectrum has increased, indicating a reorganization of the surface irons during the CO adsorption. (iii) A new intense peak centered at 2.8 Å (not corrected for phase shift) is observed.

To confirm the assignment for this new intense peak, an amplitude analysis was performed. This procedure was started by the use of the Fourier transform obtained from 3.5 to 11.5 $Å^{-1}$ which showed more separable contributions in the range 2.5 to 3.2 Å. The Fe *K*-edge EXAFS of the apical Fe fragment in $FeCo_3(CO)_{12}$ (16) was used as a reference because the different contributions from Fe–C, Fe–Co, and Fe–C–O shells were well resolved in its Fourier transform. It can be seen from Figs. 4B and C that the envelope of the amplitude obtained from the filtered oscillation in the range 2.61 to 3.07 Å is quite different from that of the Fe neighbors obtained in the range 1.84 to 2.20 Å, but is similar feature to that of the colinear Fe–C–O contribution in $FeCo_3(CO)_{12}$ (dashed line). The Fourier-filtered oscillations of K7CO were therefore obtained in the range 0.7 to 2.63 Å without any contribution from this new peak.

The amplitude of the first sphere clearly exhibits a two-shell feature (see Fig. 4A). The FEFF3.25 program allows us to distinguish C_t-scattering (terminal carbon) from O-scattering with distinct theoretical components because the nearest environment of the C_t is significantly different from that of the surface oxygen, which has six oxygen and one Al^{3+} neighbors, whatever orientation the γ-Al_2O_3 surface is in (17–20). Theoretical components and the amplitudes derived for the C_t- and O-scattering atoms used in this work are shown in Fig. 5. The results illustrate that fitting the C_t and O with a distinct approach is possible, particularly when low *k*-space (<3 $Å^{-1}$) is involved.

The best fits of the Fourier-filtered Fe *K*-edge EXAFS of K7CO and the Fourier transform are summarized in Fig. 6 and Table 1. The best fits indicate the following:

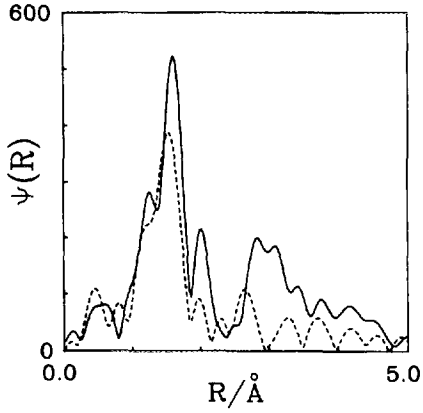

FIG. 3. Fourier transform of the Fe *K*-edge EXAFS of K7CO (solid line) compared with K7 (dashed line).

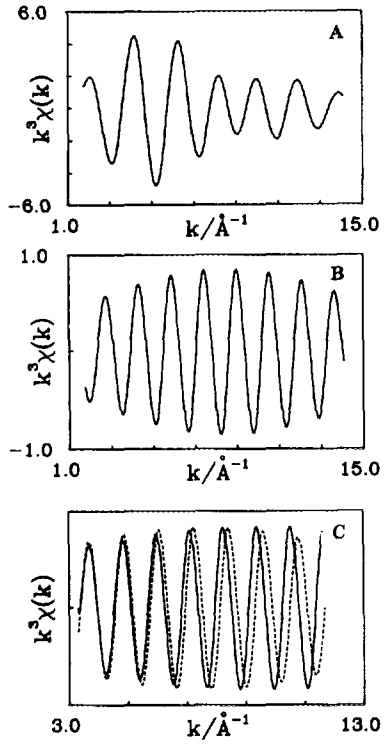

FIG. 4. Fourier-filtered Fe *K*-edge EXAFS from the peak in the ranges (A) 0.95 to 1.87 Å, (B) 1.84 to 2.20 Å, and (C) 2.61 to 3.07 Å in K7CO. C is compared with that from the Fe–C–O contribution in $FeCo_3(CO)_{12}$ (dashed line).

1. On average, a Fe site contains two C_t neighbors at 1.84(3) Å and four oxygens at 1.96(1) Å. However, the EXAFS study of K7 shows that the coordination number of surface oxygens is 3. In accordance with the infrared absorptions at 1556, 1542, 1520 cm^{-1}, the remaining scattering contribution might therefore reasonably be assigned to a triply bridged carbon atom (C_b), which connects with the three iron atoms with an average bond length of 1.96 Å. This value is comparable to that of

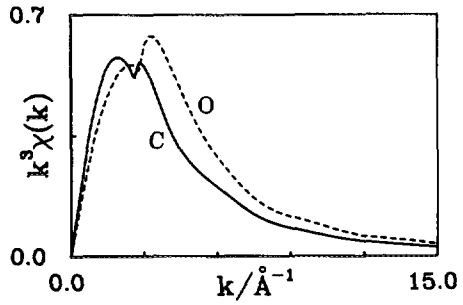

FIG. 5. Theoretical amplitudes of the C_t- and O-scattering atoms calculated by the FEFF3.25 program. Theoretical components (*R* in Å) for central Fe, CN = 8; C_t, CN = 2, *R* = 1.84; and O, CN = 8, *R* = 1.96.

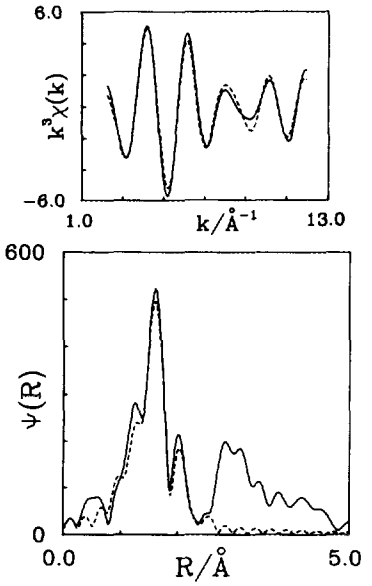

FIG. 6. Best fits (dashed lines) to the Fourier-filtered Fe *K*-edge EXAFS of K7CO and to the Fourier transform.

Fe–μ_3-C in $Fe_4(CO)_{13}^{2-}$, 2.00(3) Å, on average (21). This latter complex has a weak infrared band at 1661 cm^{-1} arising from the μ_3-CO stretching vibration (22). Because the Fe_3 ensemble on the K7CO is significantly stabilized by the surface, a much lower carbonyl stretching vibration is not surprising and may imply a *d*-electron-rich Fe_3 ensemble (23).

2. The two Fe neighbors at 2.48(6) Å suggest a more stable Fe_3 core formed on the surface. The bond length is also comparable to that in the basal $Fe_3(\mu_3$-CO) fragment of $Fe_4(CO)_{13}^{2-}$, 2.50(1) Å on average, but significantly different from that in K7, 2.66(5) Å on average. The disappearance of the Fe neighbors at 2.73 Å on K7 implies that the rearrangement is achieved by moving this Fe atom to a position centered at 2.48 ± 0.06 Å. This shows a considerable effect of CO adsorption on the surface iron rearrangement within an ensemble, changing from an isosceles triangle on K7 to an approximately equilateral trian-

TABLE 1

Fe *K*-edge EXAFS-Derived Coordination Number (CN), Shell Radius (*R*), and Debye–Waller Factors (DW) for Each Shell of K7CO by the Best Multiple Shell Fits to Fourier-Filtered Data in the Range 0.71 to 2.63 Å with the Weight of k^3

Shell	CN	*R* (Å)	DW (Å^{-1})	*R* factor
Fe–C_t	2.1	1.84(3)	0.003	0.15
Fe–O, Fe–C_b	4.2	1.96(1)	0.005	
Fe–Fe	1.7	2.48(6)	0.016	

gle on K7CO. This means that the adsorption of CO is beneficial to retaining the iron ensembles.

3. In comparison with the Fe–C_t bonds in $Fe_3(CO)_{12}$ [1.83 Å on average by EXAFS (5), 1.82 Å by single-crystal analysis (24), ν_{CO}: 2108(sh), 2048(s), 2013(s, br), and 1984(sh) cm^{-1} for terminals], assignment of the absorptions at 2047 and 2014 cm^{-1} to the terminally adsorbed carbonyls is reasonable. Thus, the surface species on K7CO can be described as $Fe_3(CO)_6(\mu_3\text{-}CO)/Al_2O_3$.

3. Surface Coordinate Geometry

It is noteworthy not only from this work but also from the results of K7 before and after use that the iron atom radius of 1.24 Å, the same as that in α-Fe metal, and the Fe–O bond length of 1.96 Å do not agree with the ionic radius of O^{2-}, which is 1.32 Å. If the oxygens in the surface species were O^{2-}, it would suggest that the irons are ferrous cations (25). However, several experimental findings, such as the visible color change elicited when the catalyst is exposed to air under working conditions ($CO:H_2 = 1:2$, 473 K) (5) and the high activity in CO adsorption presented here, argue against this suggestion. Furthermore, if the irons were oxidized by OH^- or water in the initial step, they cannot be reduced in the CO adsorption even under reaction conditions (26). In fact, several studies of $Fe_3(CO)_{12}$ supported on hydroxylated alumina (27) or carbon black (28) have indicated clearly that the presence of hydroxyl groups stabilized the zero-valent iron carbonyl cluster and its derivatives.

A comparative Fe *K*-edge XANES study reveals that the zero-valent iron atoms in the carbonyl and related clusters usually give a greater E_0, such as 12.4 eV in $Fe_2(CO)_9$ and 14.4 eV in $Fe_3(CO)_{12}$ and $Fe_5C(CO)_{15}$. However, iron cations in oxides give a small E_0, such as 9.9 eV in bulk Fe_2O_3 and 12.9 eV in bulk Fe_3O_4. Two oxidized samples, namely, FeO/Al_2O_3 derived from the K7 by further treatment in air at 923 K and Fe_2O_3/Al_2O_3 prepared by a conventional method (29), were also investigated, as shown in Fig. 7. The derivative spectra reveal E_0 values of 11.0 eV for the former and 9.5 eV for the latter. Figure 7 also reveals an E_0 of 14.0 eV for both K7CO and K7. It is directly evident that the iron atoms on both K7CO and K7 are in the zero-valent state. A much weaker 3*d* feature of K7CO is thought to be caused by the more symmetrical, *d*-electron-enriched Fe_3 core, the same as that observed by the infrared absorptions of 1560 to 1520 cm^{-1}.

On the other hand, the changes in the radius of the oxygen are so common that in most cases they are ignored by researchers. For example, the reaction of $Fe_3(CO)_{12}$ with hydroxylated alumina results in the formation of $HFe_3(CO)_{11}^-/Al_2O_3$ (30) and then causes the formation of highly dispersed Fe/Al_2O_3 (31). In the reaction steps, the

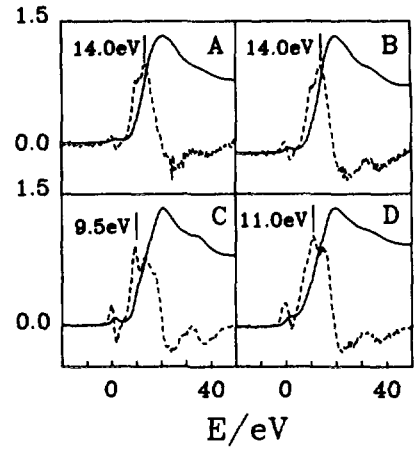

FIG. 7. Fe *K*-edge XANES spectra of (A) K7CO (the Fe/Al_2O_3 saturated with CO); (B) K7 (freshly prepared Fe/Al_2O_3, 0.9 wt% Fe); (C) well-defined Fe_2O_3/Al_2O_3; (D) FeO/Al_2O_3 (Fe/Al_2O_3 oxidized in air at 923 K).

oxygens in Al–O–H, Al–O–C–Fe, and Fe–O–Al are considerably different. Generally, an oxygen of radius 1.32 Å is rarely found in zero-valent, oxygen-containing organometallic compounds. A group of three O^{2-} ions rather than that of CO (32, 33) would polarize the iron atoms. As the bonding of Fe–O changes from ionic to covalent, the radius of the surface oxygen may be much smaller than those observed on an ideal Al_2O_3 surface. In view of these considerations, we audaciously propose that it is not right to consider the surface oxygen as O^{2-} ions (34). EXAFS results suggest a small surface oxygen in a size which may be equal to the value in the OH^- of water. In this case, each of the surface oxygens (O_S) may offer only one electron to the Fe site. If introducing the concept of coordination chemistry to a surface complex is acceptable, with the addition of the other three electrons, the species can be formulated as $[Fe_3(CO)_6(\mu_3\text{-}CO)(O_s)_6(\mu_3\text{-}O_s)]^{3-}$, a molecular anion with C_{3V} symmetry ionically bound to the Al^+ cationic site, as shown in Fig. 8. The Fe–μ_3–C–Fe angle is calculated to be about 80° and that between the Fe–μ_3–C bond and the Fe_3 plane is about 42°.

4. Surface Structure/Catalytic Activity Relationship

Based on the stability of the $Fe_3(\mu_3\text{-}C)(\mu_3\text{-}O)$ core, it seems possible to conclude that the lower CO stretching frequency implies a greatly weakened C–O bond which would lead to a higher probability of bond cleavage on the Fe_3 ensembles. In comparison with the structure of the $Fe_3(\mu_3\text{-}CCO)$ fragment in $Fe_3(CO)_9(CCO)^{2-}$ (35, 36), formation of an active intermediate with a μ_3 carbide ligand from the μ_3-CO on K7CO is geometrically allowed under this condition. However, any intermediate derived

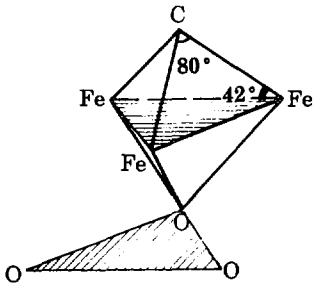

FIG. 8. Structural illustration of a $Fe_3(\mu_3\text{-}C)(\mu_3\text{-}O)$ core on the Al_2O_3 surface. Parameters used are Fe–O, 1.96 Å; Fe–C, 1.96 Å; Fe–Fe, 2.48 Å; and O···O, 2.85 Å. The Fe_3 plane is proposed to be parallel to the three oxygens labeled in the picture.

from such a stable precursor is thought to be unlikely to give high activity in the conversion of CO. A comparative study of CO hydrogenation over K7 catalyst shows that on increasing the temperature between 473 K and 623 K in 50 K steps, a higher activity was immediately observed for each point, but was no longer detectable over a 15-min period. Similarly, rapid exchange of the gas phase with H_2 instead of the syngas under the working conditions also caused an immediate higher yield. In both cases, because of the higher surface concentrations of CO and related derivatives, not only was the conversion of CO increased from 1.5 to 2.0–3.5%, but the higher selectivity to lower olefins was also reproduced. In contrast, increasing the syngas pressure was not crucial. These results agree closely with those predicted previously and imply that the higher activity occurring on Fe/Al_2O_3 catalyst is attributable to the desorption of the intermediates formed on the Fe sites, and that the higher selectivity is attributable to the rapid desorption of a unique intermediate structurally derived from the Fe_3 ensembles. The results presented in this paper strongly indicate that $Fe_3(CO)_6(\mu_3\text{-}CO)/Al_2O_3$ is probably the precursor of the unique intermediate. This seems to be why the cluster-derived catalyst of Fe/Al_2O_3 always shows a poor conversion in the hydrogenation of CO, even though a high selectivity to lower olefins can be obtained and/or the aggregation of the three-iron ensembles can be diminished significantly (5, 37–39).

CONCLUSION

The surface species $Fe_3(CO)_6(\mu_3\text{-}CO)/Al_2O_3$ has been obtained from the cluster-derived catalyst Fe/Al_2O_3 by saturation with CO. The structure is supported by the analyses of infrared results and X-ray absorption fine structure. Geometric considerations suggest that the species is inlaid into the surface and stabilized by the $Fe_3(\mu_3\text{-}C)(\mu_3\text{-}O)$ core. Introducing the basic concept of coordination chemistry to the surface approach, the species can be described as $[Fe_3(CO)_6(\mu_3\text{-}CO)(O_s)_6(\mu_3\text{-}O_s)]^{3-}$, a molecular anion with C_{3v} symmetry ionically bound to the Al^+ cation. It is clear that the formation of a μ_3 carbide ligand from the μ_3-CO is geometrically allowed, and that the reconstruction of the surface oxygens is geometrically needed, particularly when terminal oxygens are loosely bound to the Fe sites.

ACKNOWLEDGMENTS

The project was supported by the National Natural Science Foundation, China. We are grateful to the Photon Factory in Tsukuba, Japan, for use of the BL-7C facilities. We also thank Dr. T. Tanaka and Professor M. Nomura for experimental assistance. The revised version of this paper was prepared in the Department of Chemistry at the University of California, San Diego, to which one of us (Y.K.) is particularly indebted.

REFERENCES

1. Deeba, M., Scott, J. P., and Gates, B. C., *J. Catal.* **71,** 373 (1981).
2. Knözinger, H., and Zhao, Y., *Faraday Discuss. Chem. Soc.* **72,** 53 (1981).
3. Muetterties, E. L., Rhodin, T. N., Band, E., Brucker, C. F., and Pretzer, W. R., *Chem. Rev.* **79,** 91 (1979).
4. Jensen, M. P., and Shriver, D. F., *J. Mol. Catal.* **74,** 73 (1992).
5. Kou, Y., Wang, H.-L., Te, M., Tanaka, T., and Nomura, M., *J. Catal.* **141,** 660 (1993).
6. Antonic, M. R., Brazdil, J. F., Glaezer, L. C., Mehicic, M., and Teller, R. G., *J. Phys. Chem.* **92,** 2338 (1988).
7. Antonic, M. R., Teller, R. G., Sandstrom, D. R., Mehicic, M., and Brazdil, J. F., *J. Phys. Chem.* **94,** 2939 (1990).
8. Rehr, J. J., Mustre de Leon, J., Zabinsky, S. I., and Albers, R. C., *J. Am. Chem. Soc.* **113,** 5135 (1991).
9. Mustre de Leon, J., Rehr, J. J., Zabinsky, S. I., and Albers, R. C., *Phys. Rev. B* **44,** 4146 (1991).
10. Lytle, F. W., Sayers, D. E., and Stern, E. A., *Physica B* **158,** 701 (1989).
11. Cox, A. D., *in* "EXAFS for Inorganic Systems," DL/SCI/R17, p. 51 Davesburg, 1981.
12. Kristoff, J. S., and Shriver, D. F., *Inorg. Chem.* **13,** 499 (1974).
13. Butts, S. B., and Shriver, D. F., *J. Organomet. Chem.* **169,** 191 (1979).
14. Wilkinson, J. R., and Todd, L. J., *J. Organomet. Chem.* **118,** 199 (1976).
15. Hodali, H. A., Arcus, C., and Shriver, D. F., *Inorg. Chem.* **20,** 218 (1980).
16. Kou, Y., Lu, J., and Yin, Y., *Acta Chim. Sin.* **48,** 873 (1990).
17. Foger, K., *in* "Catalysis: Science and Technology" (J. R. Anderson and M. Boudart, Eds.), Vol. 6, p. 231 Springer-Verlag, Berlin, 1984.
18. Iijima, S., *Surf. Sci.* **156,** 1003 (1985).
19. Reller, A., and Cocke, D. L., *Catal. Lett.* **2,** 91 (1989).
20. Chen, Y., and Zhang, L., *Catal. Lett.* **12,** 51 (1992).
21. Doedens, R. J., and Dahl, L. F., *J. Am. Chem. Soc.* **88,** 4847 (1996).
22. Farmery, K., Kilner, M., Greatrex, R., and Greenwood, N. N., *J. Chem. Soc. A,* 2339 (1969).
23. Zwart, J., and Snel, R., *J. Mol. Catal.* **30,** 329 (1985).
24. Cotton, F. A., and Troup, J. M., *J. Am. Chem. Soc.* **96,** 4155 (1974).
25. Koningsberger, D. C., and Gates, B. C., *Catal. Lett.* **14,** 275 (1992).
26. Garten, R. L., and Ollis, D. F., *J. Catal.* **35,** 232 (1974).
27. Brenner, A., and Hucul, D. A., *Inorg. Chem.* **18,** 2836 (1979).
28. Stevenson, S. A., Goddard, S. A., Arai, M., and Dumesic, J. A., *J. Phys. Chem.* **93,** 2058 (1989).
29. Ji, W., Shen, S., Li, S., and Wang, H.-L., *in* "Preparation of Cata-

lysts. V" (G. Poncelet, P. A. Jacobs, P. Grange, and B. Delmon, Eds.), p. 517. Elsevier, Amsterdam, 1991.
30. Hugues, F., Basset, J. M., Ben Taarit, Y., Choplin, A., Primet, M., Rojas, D., and Smith, A. K., *J. Am. Chem. Soc.* **104,** 7020 (1982).
31. Hugues, F., Besson, B., and Basset, J. M., *J. Chem. Soc. Chem. Commun.*, 719 (1980).
32. Bagus, P. S., Hermann, K., and Bauschlicher, C. W., *J. Chem. Phys.* **80,** 4378 (1984).
33. Bauschlicher, C. W., and Bagus, P. S., *J. Chem. Phys.* **81,** 5889 (1984).
34. Shluger, A. L., Gale, J. D., and Catlow, R. A., *J. Phys. Chem.* **96,** 10389 (1992).
35. Kolis, J. W., Holt, E. M., and Shriver, D. F., *J. Am. Chem. Soc.* **105,** 7307 (1983).
36. Hriljac, J. A., and Shriver, D. F., *J. Am. Chem. Soc.* **109,** 6010 (1987).
37. Hugues, F., Smith, A. K., Ben Taarit, Y., and Basset, J. M., *J. Chem. Soc. Chem. Commun.*, 68 (1980).
38. Keim, W., Berger, M., and Schlupp, J., *J. Catal.* **61,** 359 (1982).
39. Van der Lee, G., and Ponec, V., *Catal. Rev. Sci. Eng.* **29,** 188 (1987).